International Journal of Physical Sciences Vol. 7(27), pp. 5036-5048, 12 July, 2012
Available online at http://www.academicjournals.org/IJPS
DOI: 10.5897/IJPS12.412
ISSN 1992 - 1950 ©2012 Academic Journals

Full Length Research Paper

Measurement of sediment oxygen demand for modeling the dissolved oxygen distribution in a Subalpine lake

Wei-Bo Chen[1], Wen-Cheng Liu[2]* and Li-Ting Huang[2]

[1]Department of Bioenvironmental Systems Engineering, National Taiwan University, Taipei 10617, Taiwan.
[2]Department of Civil and Disaster Prevention Engineering, National United University, Miao-Li 36003, Taiwan.

Accepted 15 June, 2012

Sediment oxygen demand (SOD) is believed to be an important process affecting dissolved oxygen (DO) concentrations and has become an integral part of modeling dissolved oxygen (DO) in surface water bodies. Because no SOD data are measured at specific study sites, it is common for researchers to take SOD values from the literature for use in DO modeling. This paper focuses on an approach for measuring sediment oxygen demand in the laboratory using undisturbed sediment core samples in the Yuan-Yang Lake (YYL) of north-central Taiwan. The measured SOD values among six sampling stations were within the range of 0.06 to 4.50 g/m^2/day at a temperature of 20°C. The ordinary kriging method was then applied to map the spatial distribution of the monthly average SOD values, which were incorporated into a three-dimensional water quality model for simulating the dissolved oxygen distribution of the lake. The simulation results accurately reflect the field-measured DO concentrations. Model sensitivity analyses were also conducted with increasing and decreasing 30% SOD values based on the monthly average SOD in the spatial distribution. The simulated results reveal that SOD had a significant impact on the DO concentrations in the lake. The present work, with its field measurements and numerical modeling, will provide assistance in lake water quality management.

Key words: Sediment oxygen demand, dissolved oxygen, measurement, water quality model, kriging, Yuan-Yang Lake.

INTRODUCTION

Dissolved oxygen (DO) is an important indicator of water quality in rivers, estuaries, reservoirs, and lakes. The amount and distribution of DO are affected by atmospheric exchange, physical circulation, turbulence, and water temperature as well as organic activity, such as primary production, decomposition of organic matter, and other biological processes. Sediment oxygen demand (SOD) is a significant sink variable in the calculation and prediction of DO and is, therefore, an important process in accurately determining the extent of total demand.

SOD is the rate at which DO is removed from the water column in surface water bodies due to the decomposition of organic matter in the bottom sediments, and it includes both the respiration rates of benthic communities and the chemical oxidation of reduced substances in the sediment (Chau, 2002; Rasheed et al., 2006; Miskewitz et al., 2010). SOD rates observed under natural environments are the result of soluble organic substances in the water column, which are derived from naturally occurring sediments containing aquatic plants, animals, and detritus (Truax et al., 1995; Chen et al., 2000; Higashino et al., 2004; Haag et al., 2006).

There are several factors that affect the SOD rate, such as sediment age, surface area, depth of deposit, temperature, water velocity, and chemical and biological differences. The primary focus is on the biological components, such as the organic content of benthic sediment and microbial concentrations.

Many studies have been implemented on temperature and SOD, and it has been observed that temperature can have a particularly significant effect (Hanes and Irvine, 1986; Griffin et al., 1999; Otubu et al., 2006). Till date, two fundamental approaches to measuring SOD have been well documented in the literature: laboratory

*Corresponding author. E-mail: wcliu@nuu.edu.tw.

measurements of sediment core samples and *in situ* field measurements (Edberg and Hofsten, 1973). Both methods have their pros and cons. Laboratory measurements are generally more accurate than field measurements because they are performed in a more controlled environment. Murphy and Hicks (1986) concluded that current techniques of *in situ* SOD measurement are still unsatisfactory and that a universally accepted or standard method has not yet been developed.

Most SOD measurements are taken in streams, rivers, and estuaries (Ziadat and Berdanier, 2004; MacPherson et al., 2007; Utley et al., 2008; Liu et al., 2009; Miskewitz et al., 2010), with few reported measurements of lakes and reservoirs. Sommaruga (1991) took undisturbed sediment samples from Lake Ton-Ton, Uruguay, to measure SOD in the laboratory and found that the mean SOD rate was 1.24 g/m^2/day. Veenstra and Nolen (1991) conducted *in situ* SOD measurements in five southwestern U.S. lakes. They reported that the measured mean SODs in Broken Bow Lake (Oklahoma), Lake Texoma (Texas and Oklahoma), Birch Lake (Oklahoma), Pine Creek Lake (Oklahoma), and Pat Mayse Lake (Texas) are 1.49, 1.69, 3.20, 3.39, and 4.08 g/m^2/day, respectively. Recently, Gin and Gopalakrishnan (2010) performed five SOD experiments in the laboratory using undisturbed sediment collected from the Kranji Reservoir in Singapore. Their obtained SOD values ranged from 1.4 to 3.3 g/m^2/day.

The effect of SOD on the oxygen budget of an entire water system should not be underestimated, as it can be a critical sink of DO. In some water systems, SOD can account for more than half of the total oxygen demand and can play a primary role in the water quality (Matlock et al., 2003). Although the SOD value may represent a potentially major effect on the total oxygen demand within a water system, this parameter is often assumed (or estimated) in water quality models (Hatcher, 1986). Errors in this measurement could lead to inaccurate models of the water environment at great biological and financial cost.

The estimation of SOD value in the water quality model becomes the major difficulty and challenge. To resolve this difficulty, the undisturbed sediment core was taken from the field and measured the SOD in the laboratory. The measured SOD was then incorporated into the water quality model to accurately simulate the DO distribution in the water system.

Water quality modeling is one of the most common approaches used to tackle the various processes involved that lead to the rapid degradation of the ecosystems. The coupling modeling of physical and biochemical processes provides as a powerful tool for assessing quantitatively the water quality in lakes, in addition to the analysis of physical-ecological interactions among the ecological variables (Janssen, 2001; Chau et al., 2002; Arhonditsis and Brett, 2005; Wu and Chau, 2006; Zhao et al., 2006).

Several researchers have developed and applied a three-dimensional hydrodynamic-water quality model in the lakes (Jin et al., 2007; Chao et al., 2007; Mao et al., 2008; Missaghi and Hondzo, 2010).

When the water quality model was conducted to simulate the dissolved oxygen distribution in the water body, the SOD values were determined.

The objective of this study is to measure the SOD in undisturbed sediment core samples in the laboratory for the subalpine Yuan-Yang Lake (YYL). The monthly measurements of SOD were implemented from February 2009 to December 2010. The spatial distribution of SOD in YYL was constructed with the ordinary kriging method. Then, SOD values in spatial distribution were determined and incorporated into a three-dimensional water quality model, which accurately simulated time-series DO concentrations and assessed the DO distribution in YYL. Model sensitivity analyses of SOD were also performed to understand its influence on the DO concentration in the lake.

MATERIALS AND METHODS

Description of study site

Yuan-Yang Lake (YYL) is in the north-central region of Taiwan (24°35'N, 121°24'E) (Figure 1a). YYL is a small (3.6 ha), shallow (4.5 m maximum depth) lake in a mountainous catchment 1,730 m above sea level. Figure 1a shows the bathymetry of YYL. The lake and surrounding catchment (374 ha) were designated as a long-term ecological study site by the Taiwan National Science Council in 1992, and it became part of the Global Lake Ecological Observatory Network (GLEON) in 2004. The steep watersheds are dominated by pristine Taiwan false cypress [*Chamaecyparis obtusa* Sieb. and Zucc. var. *formosana* (Hayata) Rehder] forests.

YYL is slightly stained, with an average dissolved oxygen carbon concentration of 6.1 mg/L and a mean pH of 5.9. The average annual temperature is approximately 13°C (the monthly average ranges from -5 to 15°C), and the annual precipitation is more than 4,000 mm. YYL is subject to three to seven typhoons in the summer and autumn each year, during which more than 1,700 mm of precipitation may fall on the lake. The water column is stratified from early April to October. Stratification begins when the surface water temperature exceeded 11°C, and it persists until the temperature falls below approximately 13°C. The water column is usually completely mixed in the winter and is associated with intensive rainfall during the typhoon season (Kimura et al., 2012).

The total nitrogen and total phosphorus did not show significant differences, ranging from 0.2 to 0.4 mg/L and from 3.5 to 6.7 μg/L, respectively. In general, the chlorophyll *a* concentration was less than 10 μg/L. The dissolved oxygen and DO saturation concentrations ranged from 4.0 to 8.0 and 6.9 to 10.0 mg/L, respectively. Both showed similar seasonal patterns, with the summer values slightly lower than the high values in winter (Tsai et al., 2008).

Measurement

Six sampling locations (Figure 1a) were established in the YYL to measure the monthly SOD from February 2009 to December 2010. It was convenient to take the undisturbed sediment core with a boat. The undisturbed sediment samples were collected using a Phlege Core Sediment Sampler (Kahl Scientific Instrument Corporation, USA). Different volumes of sediment samples were

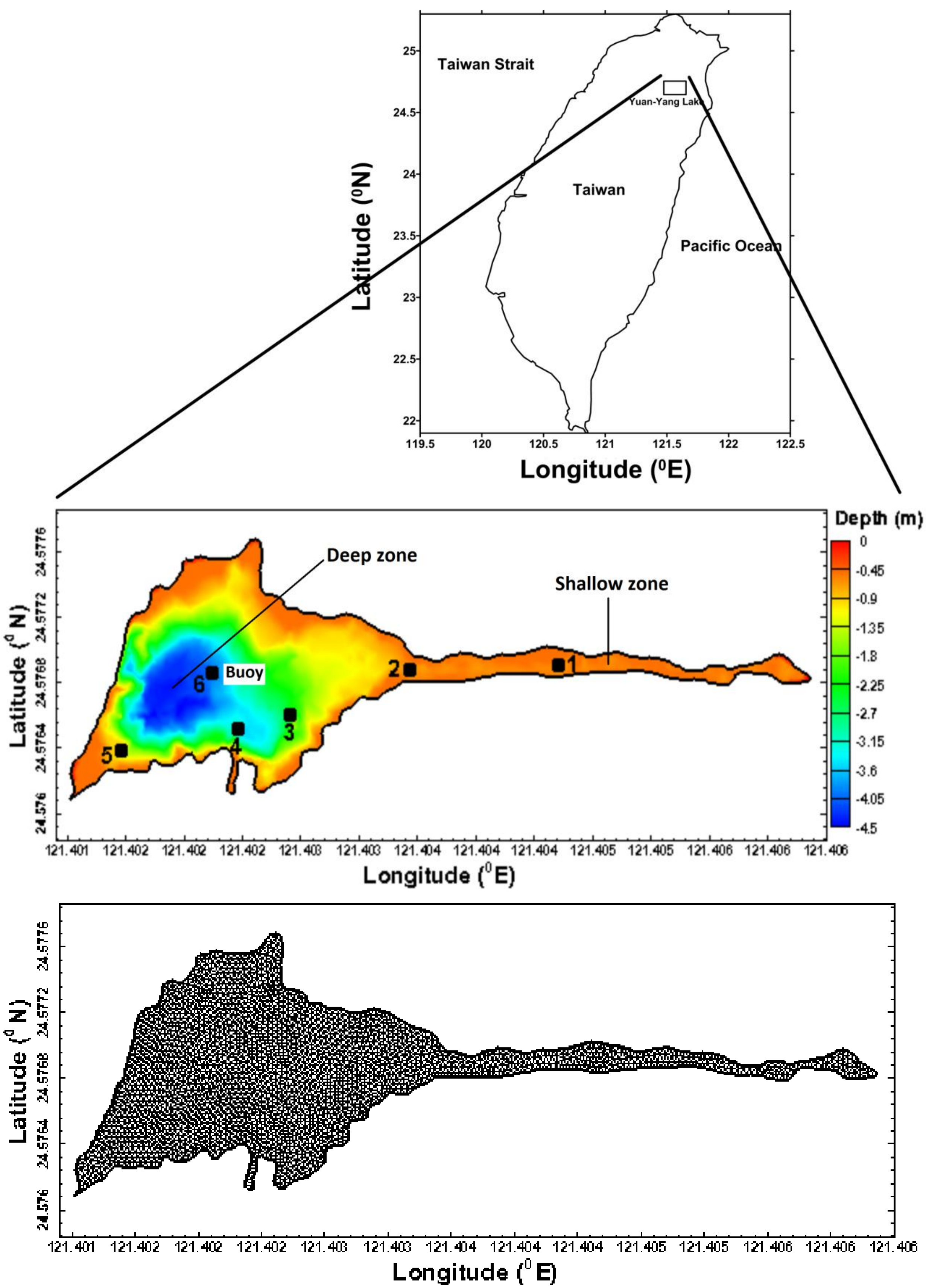

Figure 1. (a) Map of the Yuan-Yang Lake (YYL) in north-central region of Taiwan and sampling stations (■) and (b) unstructured horizontal grid of YYL for three-dimensional water quality model.

collected according to the thickness of the sediment bed. To ensure minimum disturbance, the core samples were secured in a car and transported to the Academia Sinica work station, where continuous measurement of the amount of DO in the overlying water was performed every hour with a dissolved oxygen meter (Yellow Springs Instruments Company USA, Model 550A).

Ordinary kriging

There are many different geostatistical simulation methods used to investigate spatial distributions, such as kriging, sequential indicator simulation, transition probability geostatistical simulation, and multiple point simulation. Kriging refers to a family of least-square regression algorithms that attempt to predict values of variables at locations where data are not available based on the spatial pattern of the available data. The description of kriging theory and its application are given in detail by Delhomme (1978). Ordinary kriging which has been widely applied in the geostatistical simulation is the only technique that takes into account two sources of information regarding the attributes, variables and distance between points (Saito et al., 2005).

Ordinary kriging is a linear weighted-average technique that is unbiased in regard to the expected value of residuals. The technique is widely used to find the linear unbiased estimation of a second-order stationary random field with an unknown constant mean as follows:

$$\hat{Z}(x_0) = \sum_{i=1}^{n} \lambda_i Z(x_i) \quad (1)$$

where $\hat{Z}(x_i)$ is the kriging estimation at the location; $Z(x_i)$ is the sampled values at x_i; and λ_i is the weighting factor associated with $Z(x_i)$. The estimation error (residual) is defined as:

$$R(x_0) = \hat{Z}(x_0) - Z(x_0) = \sum_{i=1}^{n} \lambda_i Z(x_i) - Z(x_0) \quad (2)$$

where $Z(x_0)$ is the true value of the regionalized variable at spatial location x_0 and $R(x_0)$ is the estimation error (residual). In an unbiased estimator, the expected value of the residual must be 0, which means that

$$E[R(x_0)] = 0 \quad (3)$$

The unbiasedness condition, which is $\sum_{i=1}^{n} \lambda_i = 1$, is obtained after operating Equation 2. In ordinary kriging, the weighting coefficient λ_i can be calculated by solving an optimization problem whereby the variance of residuals will be minimized subject to the unbiasedness condition.

The semivariogram (or variogram) is a statistical model that represents how the data vary spatially across the area of interest. The variation between points is measured using the semivariance. Pooling together pairs of data at a geographic distance h, the semivariance $\gamma(h)$ of the sample can be written as:

$$\gamma(h) = \frac{1}{2N(h)} \sum_{i=1}^{N(h)} [Z(x_i + h) - Z(x_i)]^2 \quad (4)$$

where $N(h)$ is the number of pairs of points separated by distance h. Once the semivariogram function has been computed from the sampled values at different locations, the next step is to fit parametric semivariogram $\gamma(h)$. A common method used to fit parametric semivariogram models to the sample semivariogram is the weighted least square method, as proposed by Cressie (1985). In this study, an exponential model was adopted to fit the sample semivariograms. This model parameterizes the semivariogram as follows:

$$\gamma(h) = C_o + C_1[1 - \exp(\frac{-h}{a})] \quad (5)$$

where C_0, C_1, and a are called the nugget, sill, and range, respectively.

Water quality model

Several researchers have developed structured and unstructured grids, three-dimensional hydrodynamic models to simulate the water surface elevation, current, and water temperature in the lakes. The potential advantages of an unstructured grid hydrodynamic model are significant. For example, there are issues relating to boundary conditions when bathymetry and shorelines are represented by a 'staircase' regular structured mesh. The result can be an inadvertent application of no-slip boundary conditions, and consequent problems with the transport of dense fluids along slopes. Unstructured grids also enable the use of greater mesh resolution in the direction normal to the shoreline than tangential to it where typically boundary layers develop (Pain et al., 2005). Therefore, a three-dimensional semi-implicit Eulerian-Lagrangian finite-element (that is, unstructured grid) hydrodynamic and hydrothermal model (Zhang and Baptisa, 2008) was implemented for YYL. SELFE solves the Reynolds-stress averaged Navier-Stokes equations consisting of conservation laws for mass, momentum and temperature under the hydrostatic and Boussinesq approximations to yield the free-surface elevation, the three-dimensional water velocity, and the water temperature. The water quality module was incorporated into the three dimensional hydrodynamic model.

The water quality model used in this study was built based on a three-dimensional conventional water quality analysis simulation program (call WASP5) developed originally by Ambrose et al. (1993). This program constitutes a complex interacting system of four elements: dissolved oxygen, the nitrogen cycle, the phosphorus cycle, and phytoplankton dynamics. Eight water quality components are included: dissolved oxygen (DO), phytoplankton as carbon (PHYT), carbonaceous biochemical oxygen demand (CBOD), ammonium nitrogen (NH_4), nitrate and nitrite nitrogen (NO_3), organic nitrogen (ON), ortho-phosphorus or inorganic phosphorus (OP), and organic phosphorus (OP).

A mathematical formulation of the conservation of mass can be written as:

$$\frac{\partial C}{\partial t} + \frac{\partial (uC)}{\partial x} + \frac{\partial (vC)}{\partial y} + \frac{\partial (wC)}{\partial z} = \frac{\partial}{\partial x}(A_h \frac{\partial C}{\partial x}) + \frac{\partial}{\partial y}(A_h \frac{\partial C}{\partial y}) + \frac{\partial}{\partial z}(K_v \frac{\partial C}{\partial z}) + S_c \quad (6)$$

where C is the concentration of the water quality components; u, v, and w are the water velocity components corresponding to the Cartesian coordinate system (x, y, z); A_h and K_v are the coefficients of the horizontal viscosity and vertical eddy diffusion, respectively; and S_c is the function that represents the internal source or sink of the water quality component.

Dissolved oxygen (DO)

DO is one of the most important water quality indicators. One source for DO in the water column is photosynthetic carbon fixation, which is proportional to the phytoplankton density and growth rate. Wind- or flow-induced reaeration can be either the source or sink of DO. If the DO concentration in the water column is under saturated, reaeration will act as a source for DO; otherwise, reaeration is a sink for DO. DO in the water column is diminished by the processes associated with SOD, phytoplankton respiration, nitrification, and the oxidation of carbonaceous biochemical oxygen demand (CBOD). The mathematical representation is:

$$S_c = k_{r1}\theta_{r1}^{(T-20)}(C_s - C_{DO}) - k_{d1}\theta_{d1}^{(T-20)}\frac{C_{DO}C_{CBOD}}{K_{BOD}+C_{DO}} - \frac{32}{12}k_{r2}\theta_{r2}^{(T-20)}C_{pHYT} - \frac{32}{14}2k_{ni}\theta_{ni}^{(T-20)}\frac{C_{DO}C_{NH_4}}{K_{NITR}+C_{DO}} + G_P[\frac{32}{12}+\frac{48}{14}a_{nc}(1-P_{NH_4})]C_{PHYT} - \frac{SOD_T}{D} \quad (7)$$

where a_{nc} is the phytoplankton nitrogen-carbon ratio; C_s is the DO saturation concentration; C_{DO}, C_{CBOD}, C_{NH_4}, and C_{PHYT} are the DO, CBOD, NH_4, and phytoplankton concentrations, respectively; D is the depth of the benthic layer; G_p is the phytoplankton growth rate; k_{r1} is the reaeration rate; k_{d1} is the CBOD deoxygenation rate; k_{ni} is the nitrification rate; k_{r2} is the phytoplankton respiration rate; K_{BOD} is the half-saturation concentration for the oxygen limitation of CBOD oxidation; K_{NITR} is the half-saturation concentration for the oxygen limitation of nitrification; P_{NH_4} is the ammonium preference factor; SOD_T is the sediment oxygen demand at T^0C; θ_{r1} is the temperature adjustment for the reaeration rate; θ_{d1} is the temperature adjustment for the deoxygenation rate; θ_{ni} is the temperature adjustment for the nitrification rate; and θ_{r2} is the temperature adjustment for the phytoplankton respiration rate.

Model implementation

In this study, the bottom topography data in YYL, which were measured in August 2007, were obtained from the Academia Sinica, Taiwan. The greatest depth within the study area is 4.5 m near station 6 (Figure 1a). The model mesh for YYL consists of 4,148 polygons in the horizontal direction (Figure 1b).

Fine grids, which include the mesh size ranging from 3.2 to 6.6 m, were used for YYL. The terrain-following "pure S" layers were adopted in the vertical direction, and 20 evenly spaced S-levels were used. The "pure S" representation of the model was chosen to avoid the staircase representation of the bottom and surface and, thus, a loss of accuracy. For this model grid, a large time step (Δt = 120 s) was used in simulations with no sign of numerical instability, which means 263520 time steps for a one-year simulation. A one-year simulation takes approximately 2.5 days on an Intel Core I5 PC.

RESULTS AND DISCUSSION

Sediment oxygen demand (SOD)

SOD was defined as the rate of oxygen consumption, biologically or chemically, on or in the sediment at the bottom of a water body. The DO depletion profiles in the water overlying the sediment samples collected from sampling stations (Figure 1a) are graphically presented in Figure 2; time zero represents the beginning of the experimental period. Figure 2 presents examples of measured DO profiles for January 16, 2010, at six sampling stations. The rates of oxygen consumption were calculated from the slopes along the DO versus time profiles and the area of the sediment-water interface, and the SOD was expressed as the oxygen consumption per unit interfacial area per unit time (g/m^2/day). The formula is given by:

$$SOD_T = S * V_s / A_s \quad (8)$$

where SOD_T is the sediment oxygen demand at T^0C, S is the slope of the linear portion of the usage curve, V_s is the volume of the sample, and A_s is the area of the bottom sample.

To standardize the SOD values under 20^oC, the following equation was adopted:

$$SOD_T = SOD_{20}\theta^{(T-20)} \quad (9)$$

where SOD_{20} is the SOD rate at 20°C, and θ is the temperature coefficient. Zison et al. (1978) reported a range of 1.04 to 1.13 for θ; a value of 1.065 is commonly employed.

Figure 3 presents the mean value of the measured SOD (at 20°C), which was calculated from the monthly measurement from February 2009 to December 2010. It is revealed that the lowest SOD occurred at station 1, which is located at a shallow zone in the lake (Figure 1a). Table 1 presents the measured SOD values in the various systems and compares them with the present study. The measured SOD among the six sampling stations is within the range of 0.06 to 4.50 g/m^2/day at a temperature of 20°C (Table 2), which is within the usual range compared with other systems.

Spatial estimations of SOD using ordinary kriging

Ordinary kriging was used to obtain the spatial

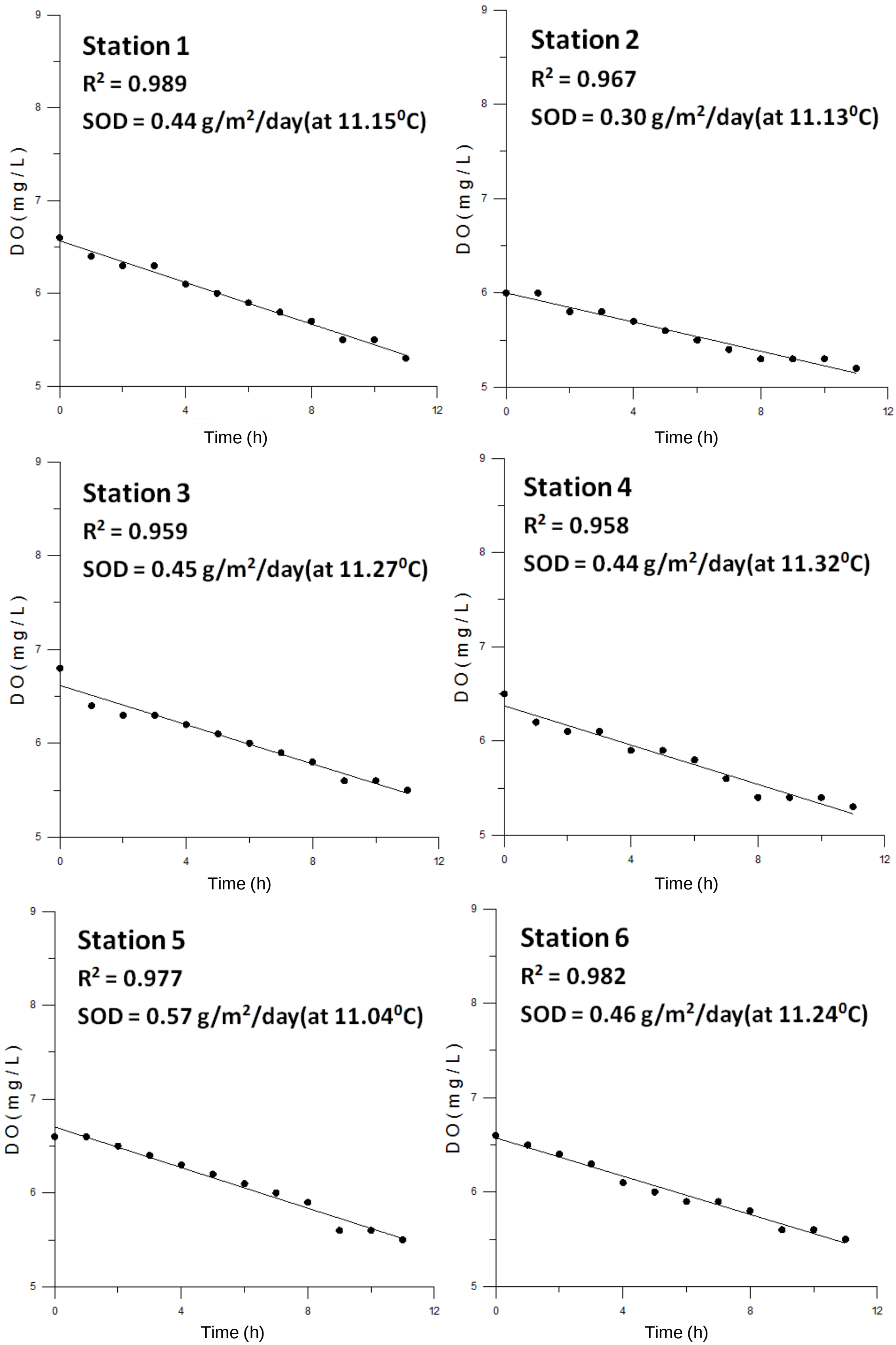

Figure 2. Consumption rate of oxygen dissolved by sediment in SOD measurement on January 16, 2010 at six sampling stations.

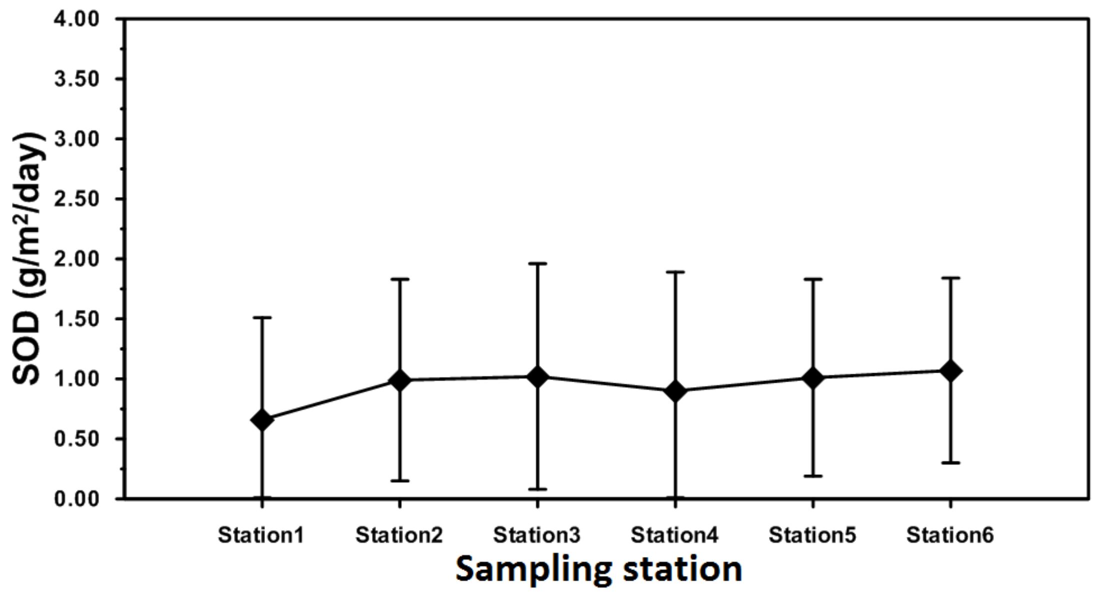

Figure 3. Measured SOD (20°C) at six sampling stations. (The mean and standard deviation values are shown in the figure).

Table 1. SOD values from literature reviews.

Location/Country	SOD ($g/m^2/day$)	Reference
Lake Ton-Ton/Uruguay	0.90~1.74	Sommaruga (1991)
Pine Creek Lake/Oklahoma	1.73~4.46	Veenstra and Nolen (1991)
Pat Mayse Lake/Texas	1.86~9.02	Veenstra and Nolen (1991)
Lake Texoma/Texas and Oklahoma	1.03~2.90	Veenstra and Nolen (1991)
Tidal Creeks, NC/USA	0~9.3	MacPherson et al. (2007)
Millstone River, NJ/USA	0.5~2.5	Miskewitz et al. (2010)
Kranji Reservoir/Singapore	1.4~3.3	Gin and Gopalakrishnan (2010)
Yuan-Yang Lake/Taiwan	0.06~4.50	This study

All measurements were corrected to 20°C.

Table 2. Statistics analysis of SOD measurement at six measured stations.

Sampling station	Station 1	Station 2	Station 3	Station 4	Station 5	Station 6
Number of samples	22	22	22	22	22	22
Mean value of SOD	0.66	0.99	1.02	0.90	1.01	1.07
Standard deviation of SOD	0.85	0.84	0.94	0.99	0.82	0.77
SOD Range	0.12~4.30	0.11~3.83	0.17~4.50	0.06~4.36	0.1~3.18	0.13~2.98

SOD: Sediment oxygen demand at 20°C ($g/m^2/day$).

distribution of SOD. The semivariogram obtained based on the monthly measured SOD for the ordinary kriging method is presented in Figure 4. The nugget, sill, and range in Equation 5 are 0.0, 1.037, and 8.01 m, respectively. The semivariance function decreases by 95% of its original value when $h = 3a$ (Wackernagel, 2003). Figure 5 shows that the monthly average SOD map is derived from the analysis of SOD data corresponding to the period 2009 to 2010. The figure shows that the lowest SOD appears at the shallow zone, while the highest appears at the deep zone.

Simulation of dissolved oxygen

The SOD rate is often assumed or estimated in water

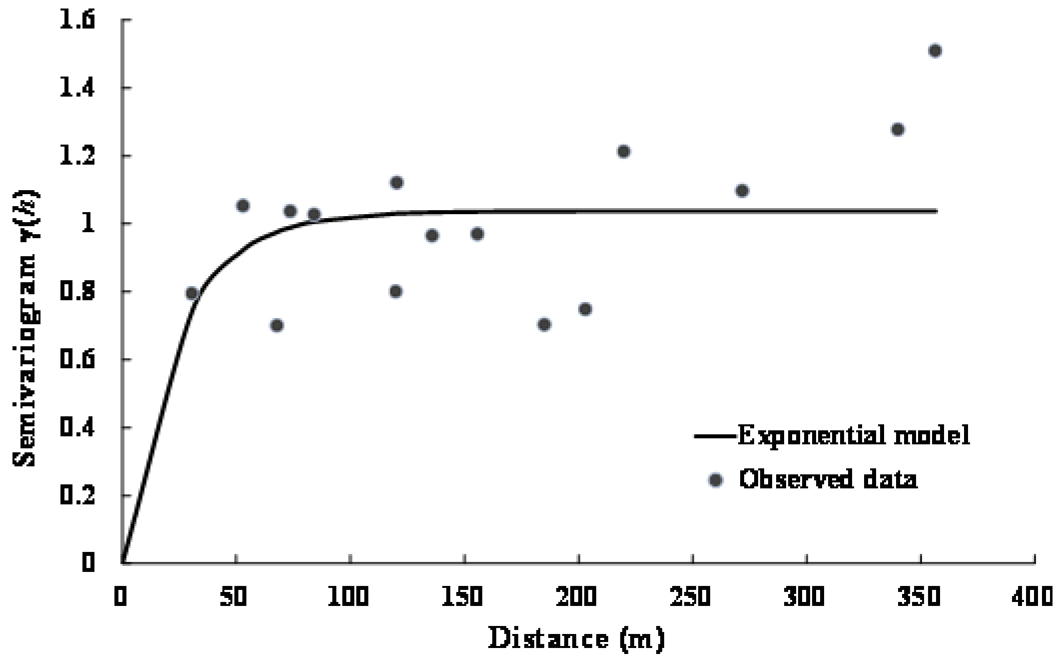

Figure 4. Variogram model used in ordinary kriging.

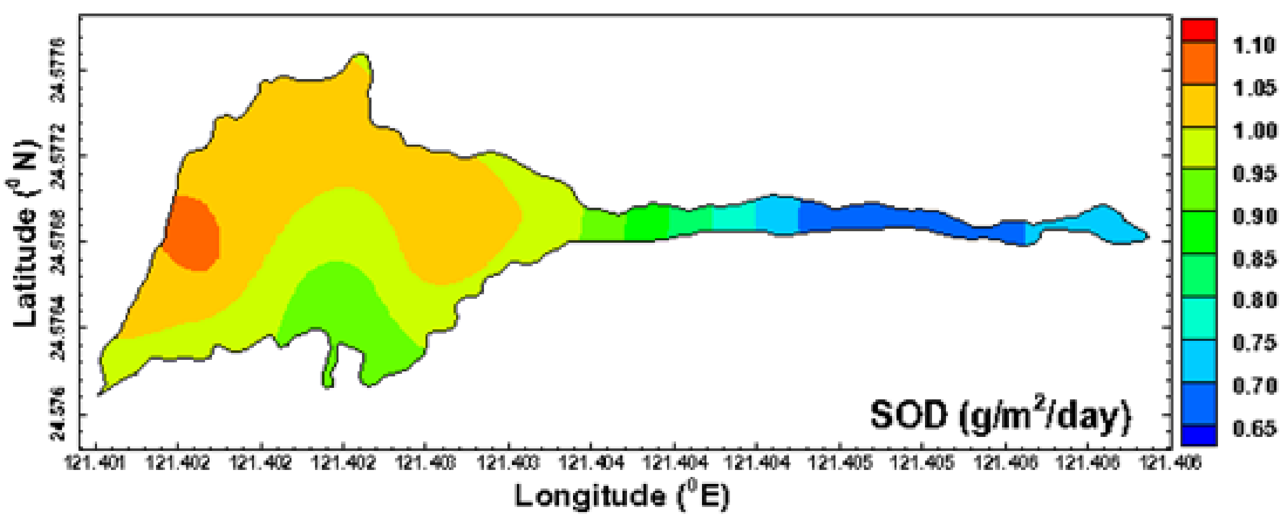

Figure 5. Monthly average SOD map based on the ordinary kriging method is derived from the analysis of SOD data corresponding to the period 2009 to 2010.

quality modeling studies that are used to set discharge limits. Errors in these assumptions can have a significant environmental and financial cost. In some river and estuarine systems, SOD accounts for as much as 50 percent of the total oxygen depletion, making SOD a critical element in water quality modeling studies. SOD is therefore an integral part of assessing the quality of water in a system (Di Toro et al., 1990).

The monthly average SOD map obtained from the ordinary kriging method (Figure 5) was used in the water quality model to simulate the spatial and temporal DO distributions in YYL. The model conducted a one-year simulation from July 2008 to June 2009.

Figure 6 presents a comparison between the model results of time-series DO and field measurements at the buoy station (that is, sampling station 6 shown in Figure 1a). The mean and standard deviation of the measured DO are shown in the figure, as are the simulated results of the time series DO concentrations at the surface and bottom layers. The model results are in reasonably good

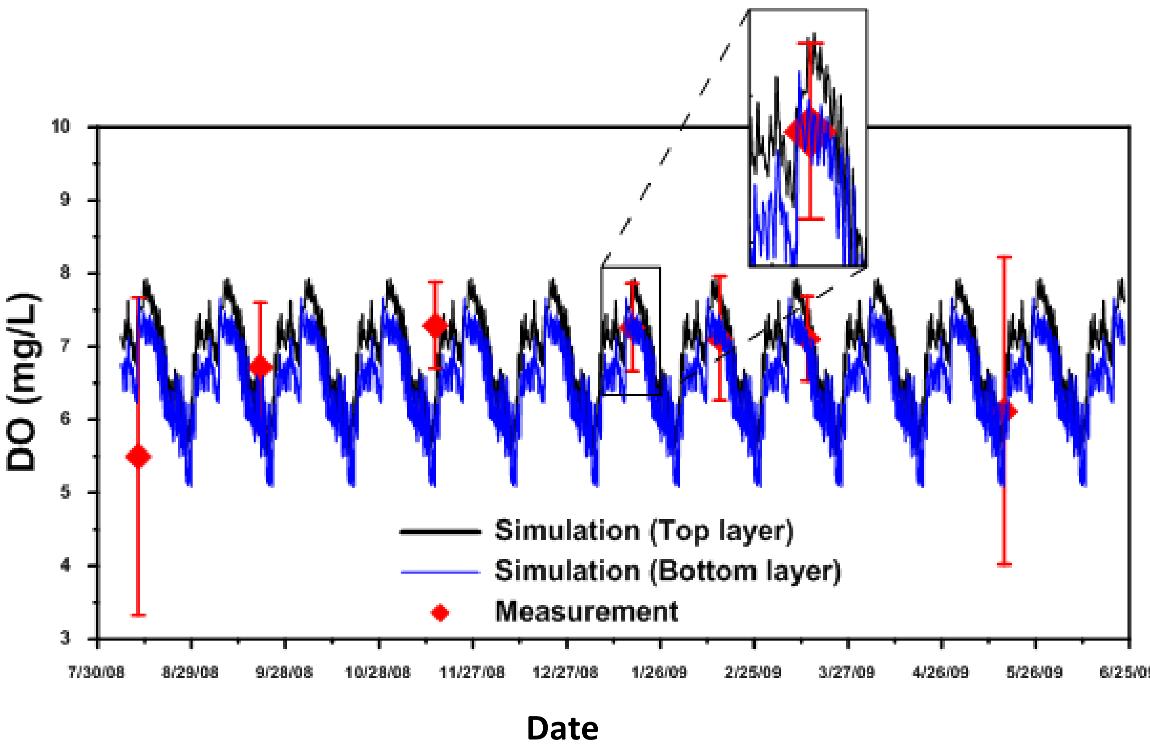

Figure 6. Comparison of measured and simulated time-series DO concentration at buoy station (presenting mean and standard deviation values in measured data).

agreement with the field measurement data in the DO with the mean plus/minus the standard deviation values. The DO concentration at the surface layer is higher than at the bottom layer. Diurnal variations of DO concentrations are clearly exhibited in the lake.

Figure 7 presents the spatial distribution of the computed DO concentrations at the surface and bottom layers. The highest DO concentration is located at the surface layer of the shallow zone (reference to Figure 1a), while the lowest DO concentration appears around the buoy station at the bottom layer, which is located at the deep zone; this is why a high SOD occurs in the deep zone, where the dissolved oxygen is difficult to transport into the deep water. Table 3 lists all coefficients (in Equation 7) adopted in the DO simulation. The sources for determining the coefficients are also present in Table 3. These coefficients are rationally determined based upon those reported by Bowie et al. (1985) and Ambrose et al. (1993). We found that theses parameters presented less sensitivity to the DO distributions in the lake.

Sensitivity analysis

A primary use of the validated model is sensitivity analysis to examine the behavior of the prototype in response to any alterations made. Sensitivity analysis is a powerful tool that can be used to improve the understanding of the present DO concentration in the lake due to the changes of SOD. The sensitivity analysis was implemented by running the model with all coefficients as in the previous section, except for the SOD values. The original base depends on the simulation of model validation presented in Figure 6. The effects of the SOD values on the DO concentration were investigated with two alternative cases: one involves monthly average SOD values (Figure 5) plus 30% SOD and the other involve monthly average SOD values minus 30% SOD.

Figure 8 presents the modeling results of the sensitivity run. Table 4 summarizes the results of sensitivity analysis. It is shown that an increase in SOD results in a decrease in the DO concentration at the surface and bottom layers (Figure 8a, b). The maximum rates for decreasing DO are 5.70 and 6.41% at the surface and bottom layers, respectively. The maximum rate means that the maximum values were calculated by the formula represented by $\frac{|C_{base}-C_{sens}|}{C_{base}}\times 100\%$, where C_{base} is the dissolved oxygen for the base run, shown in Figure 6, and C_{sens} is the dissolved oxygen for the sensitivity run, shown in Figure 8.

The decrease in SOD increases the DO at the surface and bottom layers. The maximum rates of increasing DO are 9.39 and 10.6% at the surface and bottom layers,

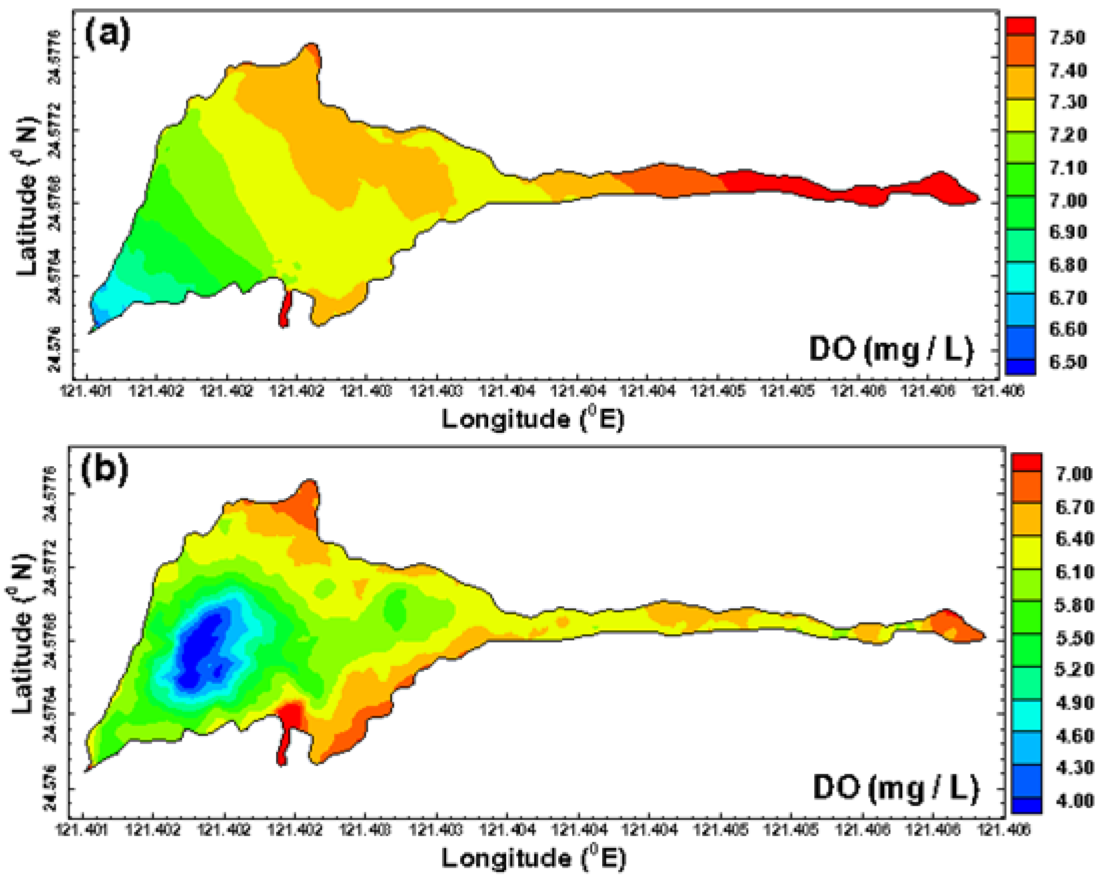

Figure 7. Computed daily-averaged dissolved oxygen of YYL at (a) surface layer and (b) bottom layer on January 1st, 2009.

Table 3. Coefficients used in the modeling of DO concentration.

Coefficients	Value	Source
k_{d1}	0.2 day^{-1}	Ambrose et al. (1993)
k_{r2}	0.1 day^{-1}	Ambrose et al. (1993)
θ_{r1}	1.028	Bowie et al. (1985)
θ_{d1}	1.047	Bowie et al. (1985)
θ_{ni}	1.080	Bowie et al. (1985)
θ_{r2}	1.080	Bowie et al. (1985)
K_{BOD}	0.5 mg O_2/L	Ambrose et al. (1993)
K_{NITR}	0.5 mg O_2/L	Ambrose et al. (1993)
a_{nc}	0.25	Ambrose et al. (1993)

respectively (Table 4). The modeling results reveal that the SOD values in the lake have a significant impact on the DO concentration.

Conclusion

The sediment oxygen demand (SOD) is considered a

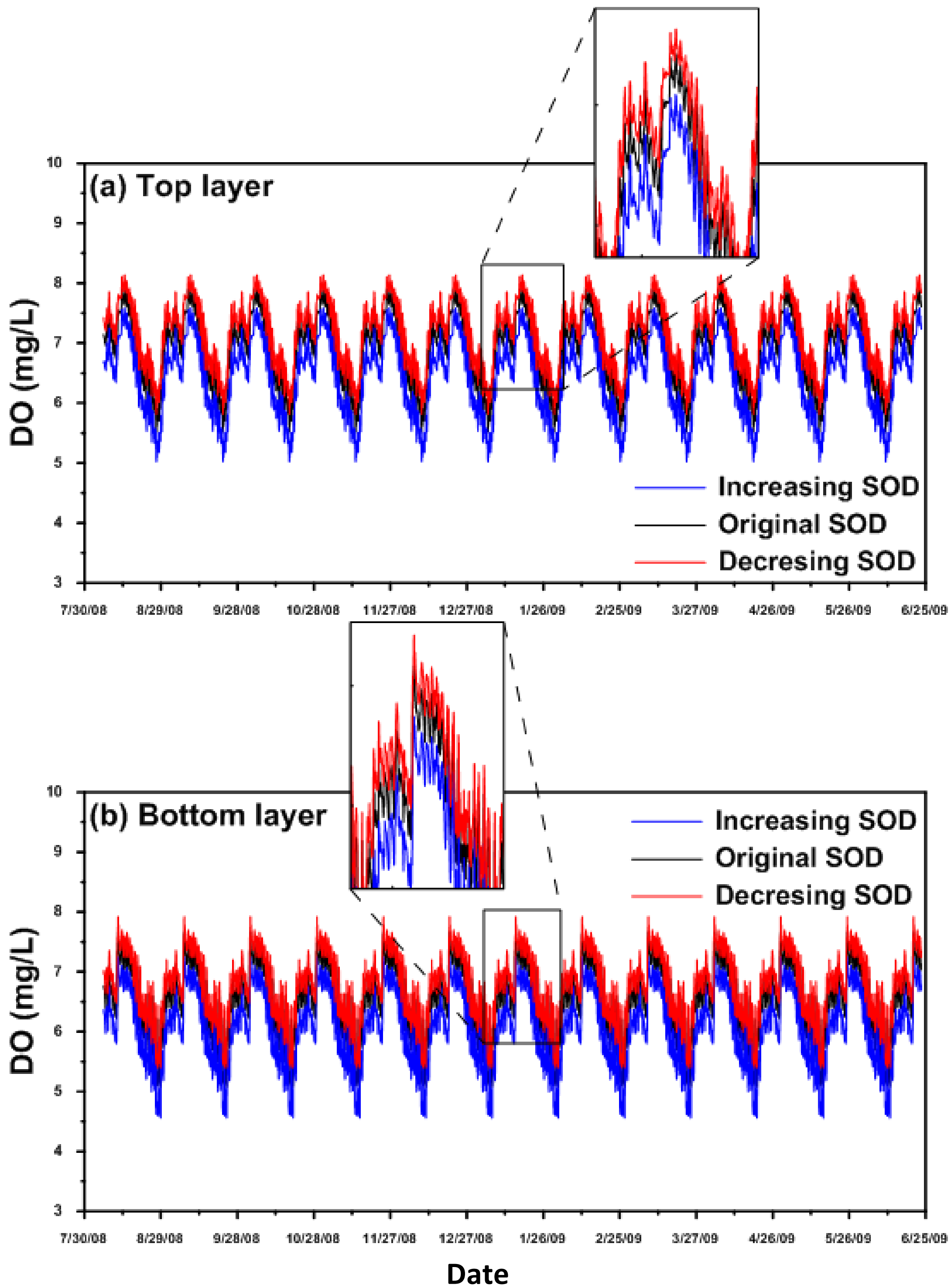

Figure 8. Sensitivity analyses running with increasing SOD and decreasing SOD at (a) surface layer and (b) bottom layer.

roughly estimated in oxygen budgets. In this study, the critical and dominant sink for dissolved oxygen (DO) in free surface systems and is often poorly investigated or monthly SOD in Yuan-Yang Lake (YYL) was measured in a laboratory setting from February 2009 to December 2010. The measured SOD values among the six sampling stations are within the range of 0.06 to 4.50 $g/m^2/day$ at a temperature of 20°C, which is within the usual range compared with other systems. The ordinary kriging method was then used to obtain the spatial

Table 4. Results of sensitivity run for increasing and decreasing SOD.

Condition	Maximum rate of dissolved oxygen concentration for surface layer (%)	Maximum rate of dissolved oxygen concentration for bottom layer (%)
Increasing 30% SOD	-5.70	-6.41
Decreasing 30% SOD	+9.39	+10.60

Minus and plus represent decreasing and increasing dissolved oxygen concentrations, respectively.

distribution of the monthly average SOD.

The monthly average SOD values in the spatial distribution of YYL were adopted in a three-dimensional water quality model to simulate the spatial and temporal variations of DO. The modeling results were in reasonable agreement with the field measurement data of the DO concentrations. Model sensitivity analyses for SOD were conducted with the validated model. The results reveal that maximum rates of DO concentration with increasing and decreasing 30% SOD values were approximately 6~11%. The measured SOD values are useful for understanding and quantifying the fluctuations of DO. The findings of this study with field measurements and numerical modeling should assist water quality management in YYL.

In the present study, the three-dimensional water quality model was developed to predict water quality conditions in the lake. This model can be extended to simulate sediment and fecal bacteria transport in the future. Moreover, the nonconventional models such as neural network and genetic programming (Muttil and Chau, 2006; Najah et al., 2011), Machine learning (Muttil and Chau, 2007), and knowledge management system (Chau, 2007) can be developed and applied to predict water quality in the lake.

ACKNOWLEDGEMENT

This study was supported by the National Science Council and Academia Sinica, Taiwan, under grant numbers NSC-96-2628-E-239-012-MY3 and AS-98-TP-B06, respectively. The financial support is greatly appreciated.

REFERENCES

Ambrose Jr. RB, Wool TA, Martin JL (1993). The water quality analysis simulation program, WASP5, Part A: model documentation. U.S. Environmental Protection Agency, Athens, Georgia p. 202.

Arhonditsis GB, Brett MT (2005). Eutrophication model for Lake Washington (USA) Part I: Model description and sensitivity analysis. Ecol. Model. 187(2-3):40-178.

Bowie GL, Mills WB, Porcella DB, Campbell JR, Pagenkopf JR, Rupp GL, Johnson KM, Chan PWH, Gherini SA, Chamberlin CE (1985). Rates, constants, and kinetics formulations in surface water quality modeling (second edition). EPA/600/3-85/040. Environmental Research Laboratory, Office of Research and Development, US Environmental Protection Agency, Athens, GA p. 455.

Chao X, Jia Y, Shields Jr. FD, Wang SSY, Cooper CM (2007). Numerical modeling of water quality and sediment related processes. Ecol. Model. 201(3-4):385-397.

Chau KW (2002). Field measurements of SOD and sediment nutrient fluxes in a land-locked embayment in Hong Kong. Adv. Environ. Res. 6(2):135-142.

Chau KW (2007). An ontology-based knowledge management system for flow and water qaulity modeling. Adv. Eng. Softw. 38(3):172-181.

Chau KW, Cheng CT, Li CW (2002). Knowledge management system on flow and water quality modeling. Expert Syst. Appl. 22(4):321-330.

Chen GH, Leong IM, Liu J, Huang JC, Lo IMC, Yen BC (2000). Oxygen deficit determinations for a major river in eastern Hong Kong, China. Chemosphere 41(1-2):7-13.

Cressie N (1985). Fitting variogram models by weighted least squares. Math. Geol. 17(5):563-586.

Delhomme JP (1978). Kriging in the hydrosciences. Adv. Water Resour. 1(5):251-266.

Di Toro DM, Paquin PR, Subburamu K, Gruber DA (1990). Sediment oxygen demand model: Methane and ammonia oxidation. J. Environ. Eng. ASCE 116(5):945-986.

Edberg N, Hofsten BV (1973). Oxygen uptake of bottom sediments studied *in situ* and in the laboratory. Water Res. 7(9):1287-1294.

Gin KYH, Gopalakrishnan AP (2010). Sediment oxygen demand and nutrient fluexes for a tropical reservoir in Singapore. J. Environ. Eng. ASCE 136(1):78-85.

Griffin Jr. DM, Bhattarai RR, Xing H (1999). The effect of temperature on biochemical oxygen demand removal in subsurface flow wetland. Water Environ. Res. 71(4):475-482.

Haag I, Schmid G, Westrich B (2006). Dissolved oxygen and nutrient fluxes across the sediment-water interface of the Neckar River, German: In situ measurement and simulations. Water Air Soil Pollut. Focus 6(1):413-422.

Hanes NB, Irvine RL (1986). New techniques for measuring oxygen uptake rates of benthal systems. J. Water Pollut. Control Fed. 40(2):223-232.

Hatcher KJ (1986). Introduction to Part 1: Sediment oxygen demand processes. In: Sediment Oxygen Demand: Processes, Modeling and Management, Hatcher KJ (ed.), Institute of Natural Resources, University of Georgia, Athens, Georgia pp.3-8.

Higashino M, Gantzer CJ, Stefan HG (2004). Unsteady diffusional transfer at the sediment/water interface: Theory and significance for SOD measurement. Water Res. 38(1):1-12.

Jassen MA (2001). An exploratory integrated model to assess management of lake eutrophication. Ecol. Model. 140(1-2):111-124.

Jin KR, Ji ZG, James RT (2007). Three-dimensional water quality and SAV modeling of a large shallow lake. J. Great Lake Res. 33(1):28-45.

Kimura N, Liu WC, Chiu CY, Kratz TK, Chen WB (2012). Real-time observation and prediction of physical processes in a typhoon-affected lake. Paddy Water Environ. 10(1):17-30.

Liu WC, Chen WB, Kimura N (2009). Measurement of sediment oxygen demand to simulate dissolved oxygen distribution: case study in the main Danshuei River estuary. Environ. Eng. Sci. 26(1):1701-711.

MacPherson TA, Cahoon LB, Mallin MA (2007). Water column oxygen demand and sediment oxygen flux: patterns of oxygen depletion in tidal creeks. Hydrobiologia 586:235-248.

Mao J, Chen Q, Chen Y (2008). Three-dimensional eutrophication model and application to Taihu Lake, China. J. Environ. Sci. 20(3):278-284.

Matlock MD, Kasprazak KR, Osborn GS (2003) Sediment oxygen demand in the Arroyo Colorado River. J. Am. Water Res. Assoc. 39(2):267-275.

Miskewitz RJ, Francisco KL, Uchrin CG (2010) Comparison of a novel profile method to standard chamber methods for measurement of sediment oxygen demand. J. Environ. Sci. Health Part A 45(7):795-802.

Missaghi S, Hondzo M (2010). Evaluation and application of a three-dimensional water quality model in a shallow lake with complex morphometry. Ecol. Model. 221(11):1512-1525.

Murphy PJ, Hicks DB (1986). *In situ* method for measuring sediment oxygen demand. In: Sediment Oxygen Demand: Processes, Modeling and Measurement, Hatcher KJ (ed.), Institute of Natural Resources, University of Georgia, Athens, GA pp. 307-330.

Muttil N, Chau KW (2006). Neural network and genetic programming for modeling coastal algae blooms. Int. J. Environ. Pollut. 28(3-4):223-238.

Muttil N, Chau KW (2007). Machine learning paradigms for selecting ecologically significant input variables. Eng. Appl. Artif. Intell. 20(6):735-744.

Najah A, El-Shafie A, Karim OA, Jaafar O, El-Shafie AH (2011). An application of different artificial intelligences techniques for water quality prediction. Int. J. Phys. Sci. 6(22):5298-5308.

Otubu JE, Hunter JV, Francisco KL, Uchrin CG (2006). Temperature effects on tubificid worms and their relation to sediment oxygen demand. J. Environ. Sci. Health Part A 41(8):1607-1613.

Pain CC, Piggott MD, Goddard AJH, Fang F, Gorman GJ, Marshall DP, Eaton MD, Power PW, de Oliveira CRE (2005). Three-dimensional unstructured mesh ocean modelling. Ocean Model. 10(1-2):5-33.

Rasheed M, Al-Rousan S, Manasrah R, Al-Horani F (2006). Nutrient fluxes from deep sediment support nutrient budget in the oligotrophic waters of the Gulf of Aqaba. J. Oceanogr. 62(1):83-89.

Saito H, McKenna SA, Zimmerman DA, Coburn TC (2005). Geostatistical interpolation of object counts collected from multiple strip transects: Ordinary kriging versus finite domain kriging. Stochastic Environ. Res. Risk Assess. 19(1):71-85.

Sommaruga R (1991). Sediment oxygen demand in man-made Lake Ton-Ton (Uruguay). Hydrobiologia 215(3):215-221.

Truax DD, Shindala A, Sartain H (1995) Comparison of two sediment oxygen demand measurement techniques. J. Environ. Eng. ASCE 121(9):619-624.

Tsai JW, Kratz TK, Hanson PC, Wu JZ, Chang WYB, Arzberger PW, Lin BS, Lin FP, Chou HM, Chiu CY (2008). Seasonal dynamics, typhoons and the regulation of lake metabolism in a subtropical humic lake. Freshwater Biol. 53(10):1929-1941.

Utley BC, Vellidi G, Lowrance R, Smith MC (2008) Factors affecting sediment oxygen demand dynamics in balckwater streams of Georgia's coastal plain. J. Am. Water Resour. Assoc. 44(3):742-753.

Veenstra JN, Nolen SL (1991). *In-situ* sediment oxygen demand in five southwestern U.S. Lakes. Water Res. 25(3):351-354.

Wackernagel H (2003). Multivariate geostatistics. Springer-Verlage, Berlin.

Wu CL, Chau KW (2006). Mathematical model of water quality rehabilitation with rainwater utilization-a case study at Haigang. Int. J. Environ. Pollut. 28(3-4):534-545.

Zhao MY, Cheng CT, Chau KW, Li G (2006). Multiple criteria data envelopment analysis for full ranking units associated to environmental impact assessment. Int. J. Environ. Pollut. 28(3-4): 448-464.

Zhang YL, Baptista AM (2008) SELFE: a semi-implicit Eulerian-Lagrangian finite-element model for cross-scale ocean circulation. Ocean Model. 21(3-4):71-96.

Ziadat AH, Berdanier BW (2004). Stream depth significance during *in-situ* sediment oxygen demand measurements in shallow streams. J. Am. Water Resour. Assoc. 40(3):631-638.

Zison SW, Mills WB, Diemer D, Chen CW (1978). Rates, constants, and kinetic formulations in surface water quality modeling. US Environmental Protection Agency, ORD, Athens, GA. USA.